High-quality unsaturated zone hydraulic property data for hydrologic applications

Kim Perkins[1] and John Nimmo[1]

Received 1 October 2008; revised 10 March 2009; accepted 5 May 2009; published 22 July 2009.

[1] In hydrologic studies, especially those using dynamic unsaturated zone moisture modeling, calculations based on property transfer models informed by hydraulic property databases are often used in lieu of measured data from the site of interest. Reliance on database-informed predicted values has become increasingly common with the use of neural networks. High-quality data are needed for databases used in this way and for theoretical and property transfer model development and testing. Hydraulic properties predicted on the basis of existing databases may be adequate in some applications but not others. An obvious problem occurs when the available database has few or no data for samples that are closely related to the medium of interest. The data set presented in this paper includes saturated and unsaturated hydraulic conductivity, water retention, particle-size distributions, and bulk properties. All samples are minimally disturbed, all measurements were performed using the same state of the art techniques and the environments represented are diverse.

Citation: Perkins, K., and J. Nimmo (2009), High-quality unsaturated zone hydraulic property data for hydrologic applications, *Water Resour. Res.*, *45*, W07417, doi:10.1029/2008WR007497.

1. Introduction

[2] Unsaturated zone hydraulic property data are important in studies related to aquifer recharge, vadose zone flow and contaminant transport, subsurface moisture dynamics and habitat quality, infiltration and rainfall-runoff relations, slope stability, effects of climate variability and change on ecosystems, surface water and groundwater interactions. They are also essential in the development of new theoretical and property transfer models (PTMs), and testing of existing models. PTMs, which can be based on simple or complex relationships among variables of interest, serve the purpose of estimating hydraulic properties from more easily measured bulk properties such as particle size distribution and bulk density. Published databases of hydraulic properties, such as those of *Holtan et al.* [1968], *Mualem* [1976], A. Nemes et al. (UNSODA model version 2.0, data set, 1999, available at http://www.ars.usda.gov/Services/docs.htm?docid=8967), and *Wösten et al.* [1999], are often used in these studies when direct measurements are not possible or when data for a large number of samples are required. Some PTM development and testing studies use these published databases [*Vereecken et al.*, 1989, 1990; *Schaap et al.*, 1998; *Hwang and Powers*, 2003], while others use unpublished data or data presented only in parameterized or graphical form [*Gupta and Larson*, 1979; *Arya and Paris*, 1981; *Wagner et al.*, 2001]. *Schaap and Leij* [1998] evaluated the effect of data accuracy on the uncertainty of PTMs and concluded that the performance of a PTM depends strongly on the data being used for calibration and testing.

[3] Desirable features of a database include (1) high reliability and precision of measurements; (2) high-quality, minimally disturbed samples; (3) a large and diverse sample population; (4) consistency in measurement techniques across the data set; (5) a full suite of hydraulic and bulk property data for each sample; and (6) ease of use. In the auxiliary material of this paper we present a data set that, though smaller in sample number than many published databases, is ideal in several ways.[1] Sample collection and preparation techniques were selected to ensure minimal sample disturbance, measurements were preformed by the same laboratory techniques under highly controlled conditions, and measurements were done by a limited number of researchers in the USGS Unsaturated Zone Flow Laboratory in Menlo Park, California. Samples are from diverse geographic, climatic, and geomorphic environments, and the data were originally generated for various research purposes including recharge estimation, simulation of variably saturated flow and contaminant transport, theoretical studies of porous media, and PTM development. Samples were from various depths, including many from below the root zone. Published data commonly include samples from shallow depths; about 80% of the samples in the data set of Nemes et al. (data set, 1999) come from depths less than 1 m. The data presented here include bulk density (ρ_b), particle density (ρ_p), particle-size distribution, saturated hydraulic conductivity (K_{sat}), hydraulic conductivity as a function of water content ($K(\theta)$), and water content as a function of matric potential ($\theta(\psi)$).

2. Site Descriptions

[4] The study areas represented by this data set, with a total of 137 individual samples, are located in the United States including the states of California, Colorado, Idaho, Indiana,

[1]U.S. Geological Survey, Menlo Park, California, USA.

[1]Auxiliary materials are available in the HTML. doi:10.1029/2008WR007497.

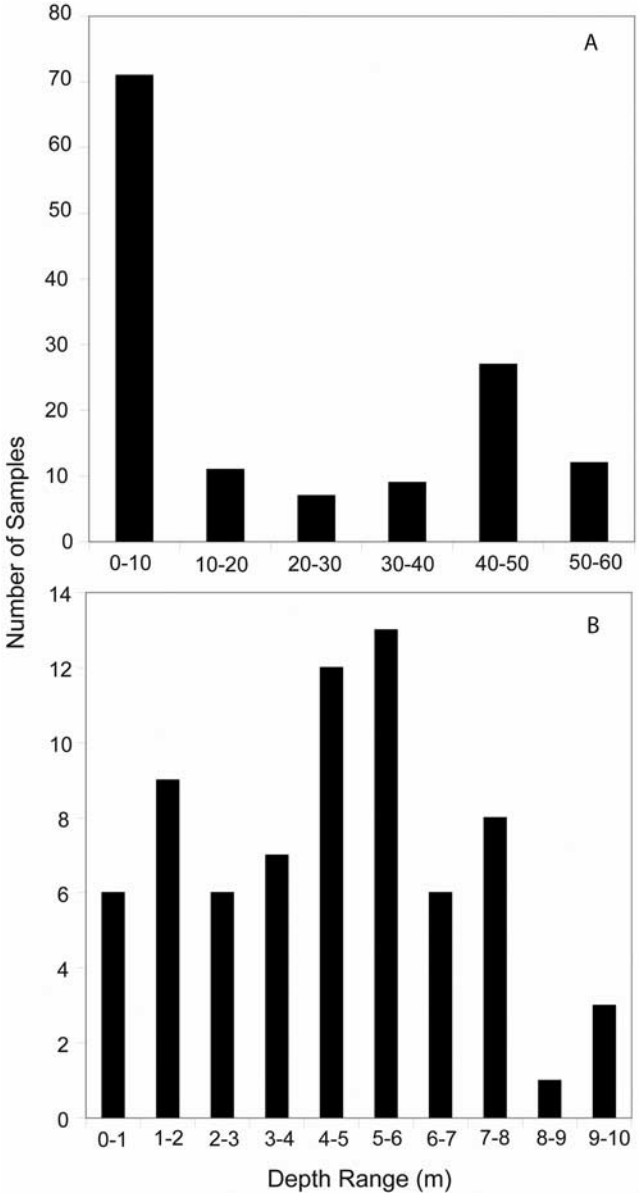

Figure 1. (a) Depth distribution of 137 core samples with (b) detailed depth information for samples from 1 to 10 m.

Maryland, Massachusetts, Montana, Nebraska, Nevada, New Jersey, New Mexico, Texas, Utah, Washington, Wisconsin, and Wyoming. The samples, which vary in depth from 0.4 to 59.9 m (Figure 1), are all minimally disturbed and encompass a wide range of environments in terms of geology, climate, and land use. Table 1 provides summary information on the individual study areas and the number of samples from each area. The auxiliary material provides additional detailed information for each site, including specific locations and depths for each sample, sampling methods used, and general information on climatic and geologic environments.

3. Methods

[5] The steady state centrifuge (SSC) method used to measure $K(\theta)$ on 133 of the 137 minimally disturbed core samples from within the various study areas is the Unsaturated Flow Apparatus (Use of brand names does not constitute endorsement by the U.S. Geological Survey) (UFA) version [*Conca and Wright*, 1998; *Nimmo et al.*, 2002] of the method originally developed by *Nimmo et al.* [1987]. The method of *Nimmo et al.* [1987] was used on 4 of the 137 samples. Most core samples, with the exception of the Middle Rio Grande Basin samples, were subcored in the laboratory using a mechanical coring device into a 4.9-cm long, 3.3-cm diameter retainer designed specifically to fit into the buckets of the UFA centrifugal rotor. The Middle Rio Grande Basin samples were smaller in diameter than the UFA retainers, therefore retainer-lining sleeves were required for a proper sample fit.

[6] The SSC method requires that steady state conditions be established within a sample under centrifugal force. Steady state conditions require application of a constant flow rate and a constant centrifugal force for sufficient time that both the water distribution and the water flux within the sample become constant. When these conditions are satisfied, Darcy's law relates K to θ and matric pressure (ψ) for the established conditions as follows:

$$q = -K(\theta)\left(\frac{d\psi}{dr} - C\rho\omega^2 r\right), \tag{1}$$

where q is the flux density (cm/s), C is a unit conversion factor of 1-cm water/980.7 dyne/cm^2, ρ is the density of the applied fluid (g/cm^3), ω is the angular velocity (rad/s), and r is the radius of centrifugal rotation (cm). If the driving force is applied with the centrifuge rotation speed large enough to ensure that $d\psi/dr \ll \rho\omega^2 r$, i.e., matric-pressure gradients that develop in the sample during centrifugation are insignificant, the flow is essentially driven by centrifugal force alone. The flow equation then simplifies to

$$q \approx K(\theta)C\rho\omega^2 r. \tag{2}$$

The ω threshold for which the $d\psi/dr$ gradient can become negligible depends on the hydraulic properties of the medium of interest. *Nimmo et al.* [1987] presented model calculations showing that the $d\psi/dr$ gradient becomes negligible at relatively low speeds for a sandy medium and at higher speeds for a fine-textured medium. This technique normally results in fairly uniform water content throughout the sample, permitting the association of the sample-average θ and ψ values with the measured K.

[7] After achieving steady flow at a given q, θ was measured by weight and ψ was measured by nonintrusive tensiometer [*Young and Sisson*, 2002] or the filter paper method [*Fawcett and Collis-George*, 1967] in cases where suctions exceeded 800-cm water. Additional dry end $\theta(\psi)$ points were measured on 17 samples using a chilled mirror hygrometer [*Nimmo and Winfield*, 2002] for suctions between 10^5 and 10^7 cm. These measurements along with the computation of K, yielded a triplet of data (K, θ, ψ) for the average water content within the sample. Repeat measurements with different q and in some cases different rotational speed gave additional points needed to define the $K(\theta)$, and $\theta(\psi)$ characteristics. There are five samples for which $\theta(\psi)$ was not measured. Three of the samples had gravel at the top surface which prohibited sufficient contact with the tensiometer and the other two simply lack that measurement.

Table 1. Study Areas and Number of Samples From Each

General Study Area	State	Number of Boreholes	Number of Samples
Merced River Basin	California	1	3
Panoche Creek	California	1	2
Western Mojave Desert	California	3	5
Northern High Plains	Colorado, Nebraska	3	17
Idaho National Laboratory	Idaho	10	46
Sugar Creek Basin	Indiana	1	1
Morgan Creek Basin	Maryland	3	3
Pomperaug River Basin	Massachusetts	3	4
Powder River Basin	Montana, Wyoming	5	6
Maple Creek Basin	Nebraska	3	4
Amargosa Desert Research Site	Nevada	2	2
Glassboro Study Area	New Jersey	7	8
Middle Rio Grande Basin	New Mexico	11	16
Trinity River Basin	Texas	6	6
Sand Hollow Basin	Utah	2	4
Granger Drain Basin	Washington	3	3
Palouse Hills	Washington	2	4
Western Lake Michigan Drainages	Wisconsin	3	3
Total		69	137

[8] K_{sat} was measured using either the standard benchtop falling head method [*Reynolds et al.*, 2002] or the falling head centrifuge method [*Nimmo et al.*, 2002] in cases where samples had very low (less than about 10^{-6} cm/s) K_{sat} values. The increased driving force allows for rapid measurement at low K_{sat} values using the equation from *Nimmo et al.* [2002]

$$K_{sat} = \frac{2aL}{A\rho g(t_f - t_i)} \ln\left[\frac{(gz_f + \omega^2 r_b^2)}{(gz_i + \omega^2 r_b^2)}\right], \quad (3)$$

where a is the cross-sectional area of the inflow reservoir (cm^2), L is the sample length (cm), A is the cross-sectional area of the sample (cm^2), t is time (s, initial and final), z is the height of water above the plane in which the sample rotates (cm), and r_b is the position of the bottom of the sample (cm).

[9] Data also include ρ_b, ρ_p, and particle-size distributions. Measurements of ρ_p were performed with the pycnometer method [*Flint and Flint*, 2002] on all core samples. Porosity was calculated using the relation $\Phi = 1 - (\rho_b/\rho_p)$ using measured ρ_b and ρ_p values. A Coulter LS-230 (Use of brand names does not constitute endorsement by the U.S. Geological Survey) particle-size analyzer was used to characterize particle-size distributions by optical diffraction [*Gee and Or*, 2002]. The range of measurement for this device is from 4×10^{-5} to 2 mm, divided into 116 size bins. Any particles above 2 mm were sieved out with American Society for Testing and Materials (ASTM) sieves (sizes 2, 2.8, 4, 5.6, 8, 11.2, 16, 22.4, and 32.5 mm) and later integrated into the size distribution results. The fraction finer than 2 mm was carefully disaggregated using a mortar and rubber-tipped pestle and then split with a 16-compartment spinning riffler to obtain appropriate representative samples for analysis.

[10] In order to perform correlation analyses, the Rossi-Nimmo junction (RNJ) model [*Rossi and Nimmo*, 1994] was used to parameterize all of the $\psi(\theta)$ data measured in the laboratory. The RNJ model consists of three functions joined at two points (defined as ψ_i and ψ_j). These functions are a parabolic function for the wet range of ψ ($\psi_i \le \psi \le 0$), a power law function [*Brooks and Corey*, 1964] for the middle range of ψ ($\psi_j \le \psi \le \psi_i$), and a logarithmic function for the dry range of ψ ($\psi_d \le \psi \le \psi_j$). The model has the following two independent parameters: (1) the scaling factor (ψ_o) and (2) the curve-shape parameter (λ). Unlike the model of Brooks and Corey, which holds θ fixed between $\psi = 0$ and the air entry pressure, the RNJ model produces a smooth curve near saturation. The curve-shape parameter λ indicates the relative steepness of the middle part of the $\theta(\psi)$ curve, described by a power law function. Larger λ values cause the drainage part of the $\theta(\psi)$ curve to change with greater sensitivity to ψ. *Morel-Seytoux and Nimmo* [1999] describe an algorithm for conversion of RNJ model parameters to *Brooks and Corey* [1964] or *van Genuchten* [1980] parameters.

[11] In the RNJ model [*Rossi and Nimmo*, 1994], the parabolic function for $\psi_i \le \psi \le 0$ is

$$\frac{\theta}{\theta_{sat}} = 1 - c\left(\frac{\psi}{\psi_o}\right)^2, \quad (4)$$

where c is a dimensionless constant calculated from an analytical function involving the parameter λ (described later) which also is dimensionless. The power law function for $\psi_j \le \psi \le \psi_i$ is

$$\frac{\theta}{\theta_{sat}} = \left(\frac{\psi_o}{\psi}\right)^{\lambda} \quad (5)$$

the logarithmic function for $\psi_d \le \psi \le \psi_j$ is

$$\frac{\theta}{\theta_{sat}} = \alpha \ln\left(\frac{\psi_d}{\psi}\right). \quad (6)$$

The dependent parameters are calculated so as to ensure continuity and smoothness at the junction points, ψ_i and ψ_j, as follows:

$$\alpha = \lambda e\left(\frac{\psi_o}{\psi_d}\right)^{\lambda}, \quad (7)$$

$$\psi_i = \psi_o\left(\frac{2}{2+\lambda}\right)^{\frac{-1}{\lambda}}, \quad (8)$$

$$\psi_j = \psi_d e^{\frac{-1}{\lambda}}, \tag{9}$$

$$c = 0.5\lambda\left(\frac{2}{2+\lambda}\right)^{\frac{\lambda+2}{\lambda}}. \tag{10}$$

A ψ_d value of -1×10^7-cm water (the pressure at which θ goes to zero) was used in the model fits for all core samples. That value is reasonable for a soil dried in an oven at 105°–110°C with 50% relative humidity in the encironment surrounding the oven [*Ross et al.*, 1991; *Rossi and Nimmo*, 1994].

[12] A simple power law function was used to parameterize the $K(\theta)$ data in order to examine possible correlations with bulk properties

$$K = m\theta^B. \tag{11}$$

A neural network analysis was performed to further assess the utility of the data for property transfer modeling. The neural network, an alternative property transfer method to predict soil properties, uses many interconnected computational nodes with which a training process is used to develop connection strengths (weights) relating input and output variables. In essence, the neural network approximates functions (linked together by weights), much like regression analysis, but has been shown to give better results where there are more than three variables [*Pachepsky et al.*, 1996]. The details of the analysis as implemented here and described by *Minasny and McBratney* [2002a] and *Minasny et al.* [2004] was performed using the Neuropack program [*Minasny and McBratney*, 2002b]. The Neuropak program allows the user to train and test a neural network using any data set and user-chosen input parameters such as bulk density and sand, silt, and clay percentages to predict the *van Genuchten* [1980] water retention parameters α and n. The accuracy of the predictions is measured using the root mean square of the residuals (RMSR) in water content at each point on the $\theta(\psi)$curve which represents the expected magnitude of the error.

4. Data Precision and Accuracy

[13] Data precision presented here is based on the precision of the measurement devices used. For example, bin limits for particle size data were taken directly from the device output or sieve size as given by the manufacturer. Precision of quantities based on weight and volume, such as bulk density, particle density, porosity and water content, were determined by the precision of the balance, caliper, or volumetric flask used.

[14] For unsaturated hydraulic property measurements it is generally impractical and therefore not common practice to replicate measurements. One reason is that no two field samples are identical, and unsaturated hydraulic properties are especially variable. Another is the cost which can be several thousand dollars per sample for high-quality unsaturated K measurements. Some measurements, such as bulk density, require that the sample be oven dried, causing irreversible alteration of properties. With laser particle size analysis the sample is in suspension and irrecoverable because of flushing of the system after each sample run. Other samples can be run from the same split of one particular core; however, the exact sample may not be run again. For reasons such as these, accuracy is evaluated here on the basis of known uncertainties of the individual measured data that contribute to the result.

[15] Uncertainty in $K(\theta)$ data measured using the SSC method arises from mechanical error associated with control of inflow rate and centrifugal driving force. According to the manufacturers of the devices used, error in inflow rate is ±2.0 percent and error in rotational speed for the centrifuge is ±20 rpm. The calculated maximum error in K due to these mechanical effects is 2%. *Nimmo et al.* [2002] discuss the assumptions inherent to the method, the importance of achieving and testing for steady state, and the possibility for net force field deviations that could affect resulting K calculations. Effects of compaction and ψ gradients on measured $K(\theta)$ have also been evaluated by *Nimmo and Akstin* [1988] and *Nimmo et al.* [1994], respectively. The combined error associated with the various issues investigated is about ±10% [*Nimmo et al.*, 2002].

[16] Uncertainties in ψ can occur as a result of error in transducer calibration, laboratory temperature fluctuations, and determination of equilibrium. On the basis of the transducer calibration data the error was on the order of 1 to 2 cm. Laboratory temperature control was maintained at ±0.5°C for all water retention measurements. Because these samples are undisturbed, ψ was monitored at the top of the samples with measures taken to prevent evaporation and equilibrium was determined by observing the pressure time series until deviations became small (on the order of a few cm). The filter paper method was used in some cases to determine ψ in the dry range; *Campbell and Gee* [1986] estimated errors in θ to be <10% at any given ψ value, on the basis of the scatter of measured data points found in the literature.

[17] For water contents determined by weighing the samples, the accuracy of the scale, the oven-dry weight, and the bulk volume affect their final values. Uncertainties in the oven-dry weight are expected to be small; samples were weighed more than once over a period of several days to verify that the weight fluctuated by less than one tenth of a gram. Bulk density measurements, upon which volumetric water content calculations depend, are subject to uncertainty arising from irregular surfaces, which were accounted for by taking several measurements at various locations using a depth micrometer, the average value of which affects the length dimension for the volume of a cylinder. Errors in bulk volume calculation were less than 1–2%.

[18] Errors in particle size distributions are more difficult to quantify. In addition to limitation in the accuracy of weight, particle shape, orientation, sample size, and time of shaking are factors known to cause errors in the determination of particle sizes by sieve analysis. Sieves generally measure the intermediate axis of a particle while optical and sedimentation methods for particle size are based on the assumption that all particles have the same density and are spherical in shape.

5. Results and Discussion

[19] Data sets for each of the 137 samples include ρ_b, ρ_p, particle-size distribution, K_{sat}, $K(\theta)$, and $\theta(\psi)$. Some data are missing for a few samples; 13 samples lack K_{sat} and 5 lack $\theta(\psi)$ measurements. All data, along with curve-fit parameters

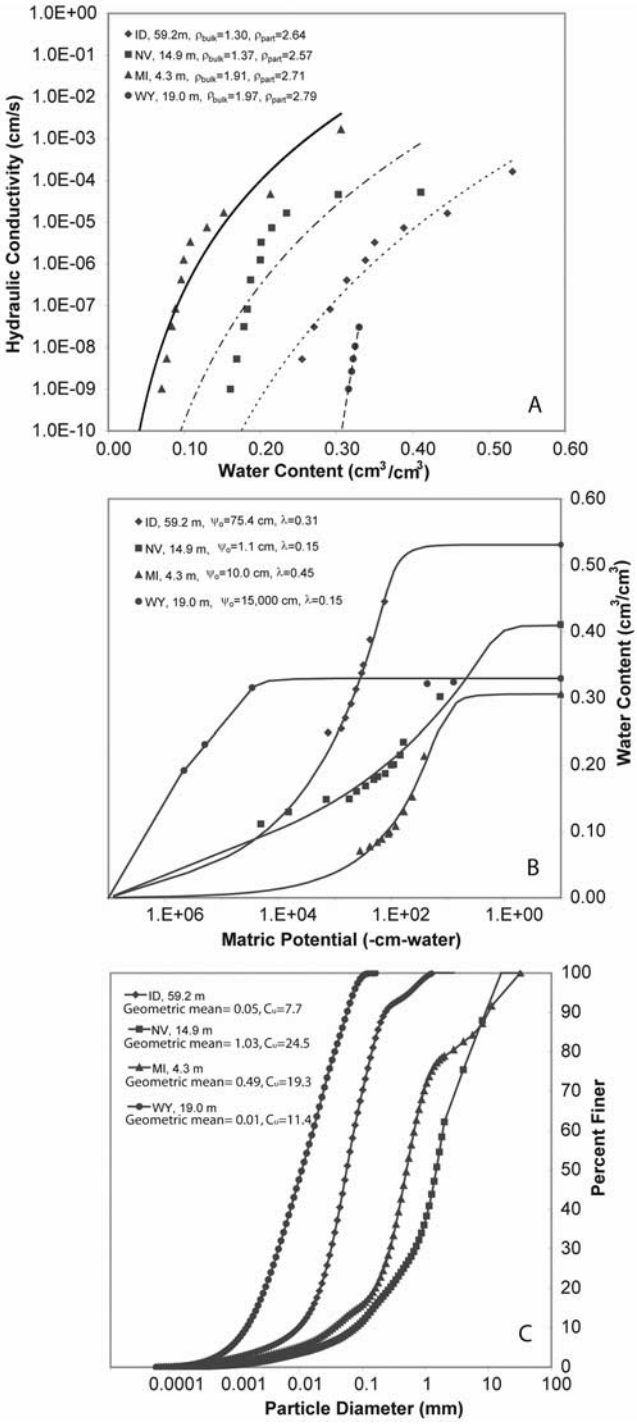

Figure 2. Example data sets for samples from Idaho, Nevada, Michigan, and Wyoming including (a) unsaturated hydraulic conductivity, bulk density, and particle density; (b) water retention and the *Rossi and Nimmo* [1994] junction model parameters ψ_o and λ; and (c) particle size distribution and geometric mean and uniformity coefficient.

and particle size statistics (arithmetic and geometric mean, median, geometric standard deviation, and the uniformity coefficient ($C_u = d_{60}/d_{10}$)), are in the auxiliary material.

[20] Figure 2 shows examples of complete data sets for four samples from Idaho, Nevada, Michigan, and Wyoming. In several ways these four data sets illustrate why many sorts of diversity are important in a database with any hope of being representative of unsaturated zone materials in general. The Wyoming sample is very dense and fine textured, as can reasonably occur at its 19-m depth but is difficult to imagine in a near-surface sample; its sensitivity of K to θ is extremely high, and its water content remains high over a large range of ψ (an air entry value read off the retention curve would be about -30 bars). Yet there is no geologic reason for such a material not to occur or even to be prevalent in some deep unsaturated zones. Such materials are likely underrepresented in existing databases because of the difficulty of obtaining such a sample and measuring its hydraulic properties. The Michigan sample provides an interesting comparison in that it similarly is compacted to high bulk density but has coarser texture. Both $K(\theta)$ and $\theta(\psi)$ of Michigan are far removed from those of Wyoming, suggesting an overriding role of texture in determining the hydraulic properties of these two samples. Curves for the Idaho and Nevada samples fall mostly between those for Wyoming and Michigan with relative positions corresponding to the coarseness of their texture. The effect of bulk density is most apparent in the wet portion of the retention curves, with the obvious effect of directing the near-saturated water contents to the porosity of the medium. Collectively these results suggest that property transfer models based on texture and porosity might be particularly effective for samples from depths of at least 4.3 m.

[21] The data were analyzed for correlations between hydraulic and bulk properties that may be useful in property transfer modeling. The variables examined for correlations include sample depth, ρ_b, particle size statistics (geometric mean, median, geometric standard deviation, and C_u), K_{sat}, parameterized $K(\theta)$, and parameterized $\psi(\theta)$. Because all of these variables, except for sample depth and ρ_b, span several orders of magnitude, logarithmic transformations were used.

[22] The SSC method used for measuring $K(\theta)$ normally allows the operator to determine the K values a priori for which the corresponding θ values are measured. Many of the samples had measured points at precisely the same K values which facilitated additional correlations. In particular, three values of K were common among many of the following samples: 1×10^{-6} cm/s (61 samples), 3×10^{-8} cm/s (79 samples), and 5×10^{-9} (76 samples). The water contents (in terms of percent saturation) at those particular K values were examined for correlations with bulk properties.

[23] Many of the bulk properties, including sample depth, ρ_b, geometric particle size standard deviation, and C_u, were uncorrelated (as indicated by low R^2 values) with any of the hydraulic properties (Table 2). There were some variables with moderate correlations with the geometric mean or median particle diameter including the RNJ model ψ_o parameter (Figure 3a) and percent saturation at all three of the common K values (Figure 3b). Additionally, there was a moderate correlation between the $K(\theta)$ α parameter and RNJ model λ parameter ($R^2 = 0.474$, Figure 4a) and between the $K(\theta)$ parameters α and m ($R^2 = 0.680$, Figure 4b). Because $\psi(\theta)$ is much easier to measure then $K(\theta)$, it would be useful if λ could be used to predict $K(\theta)$. The α parameter was better predicted ($R^2 = 0.474$) by the simple relationship than the m parameter ($R^2 = 0.274$) (Figure 5). Thus these results are

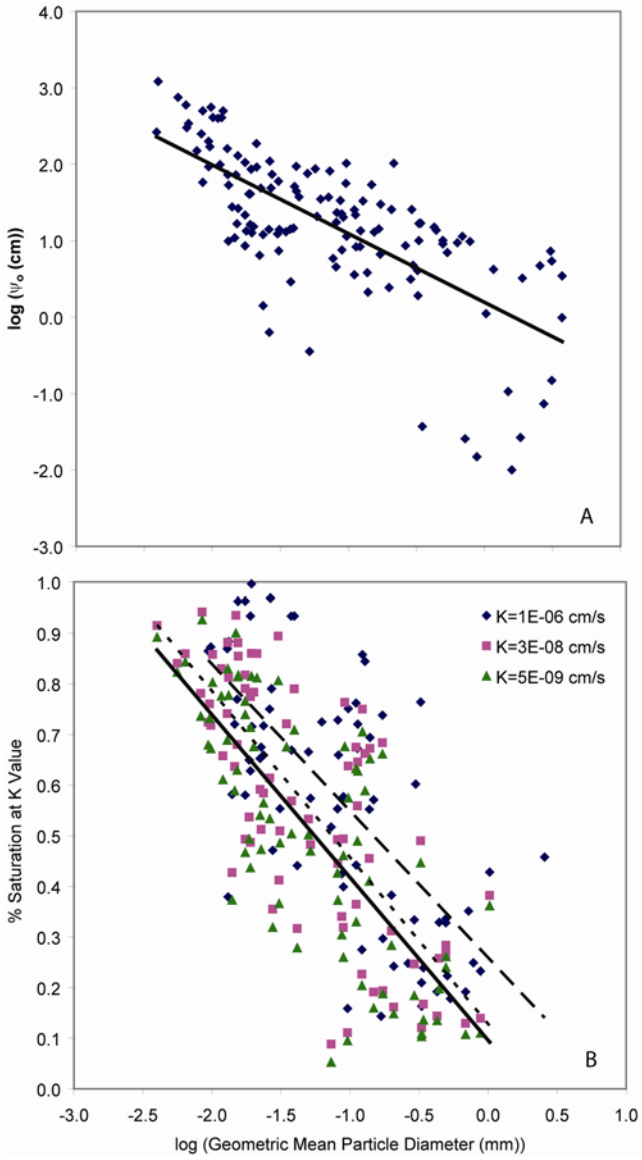

Figure 3. Correlations (a) between the Rossi-Nimmo junction model parameter ψ_o and geometric mean particle diameter and (b) between percent saturation at three common K values and geometric mean particle diameter.

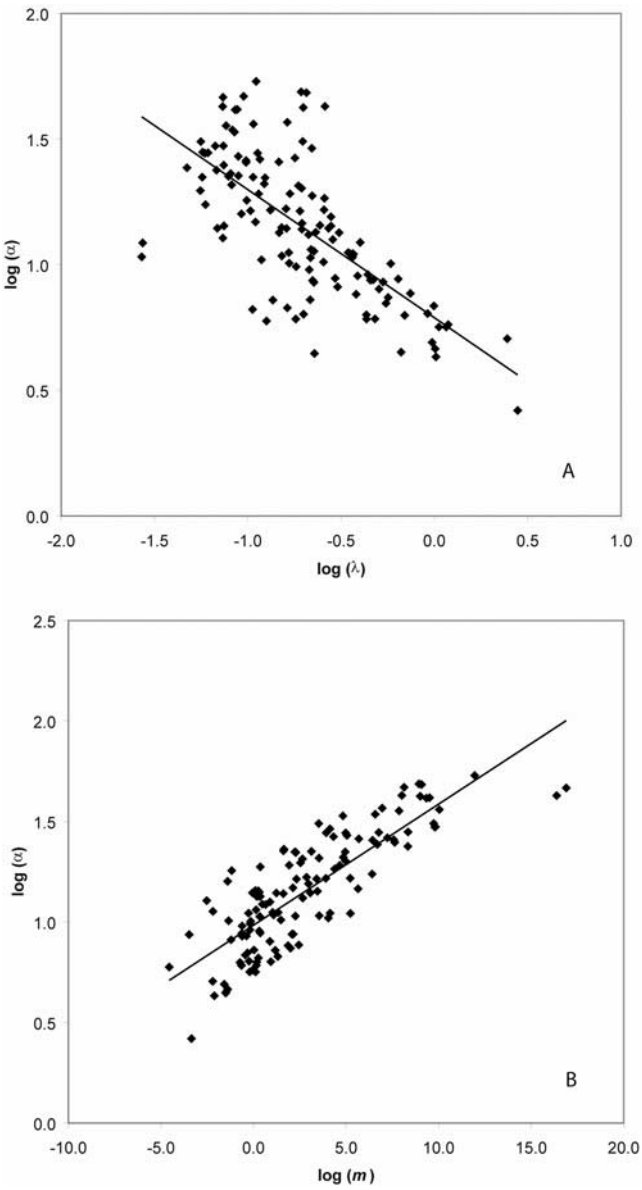

Figure 4. Correlations (a) between the $K(\theta)$ fit parameter α and the Rossi-Nimmo junction model parameter λ and (b) between $K(\theta)$ fit parameters α and m.

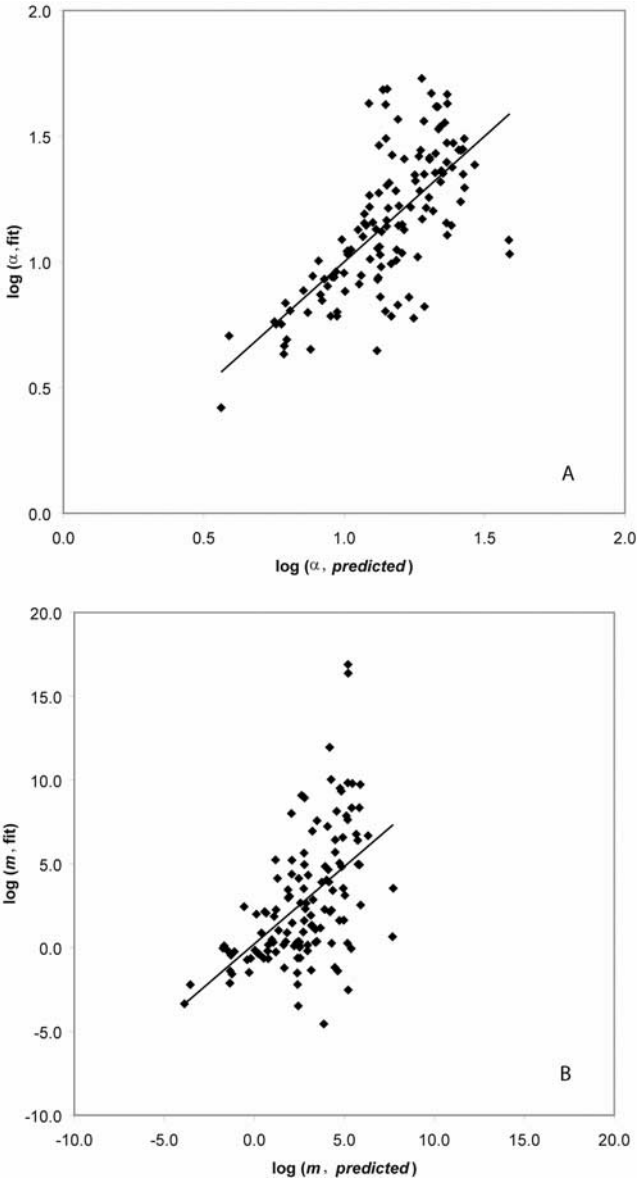

Figure 5. Correlations (a) between the fit and predicted $K(\theta)$ parameter α and (b) between the fit and predicted $K(\theta)$ parameter m.

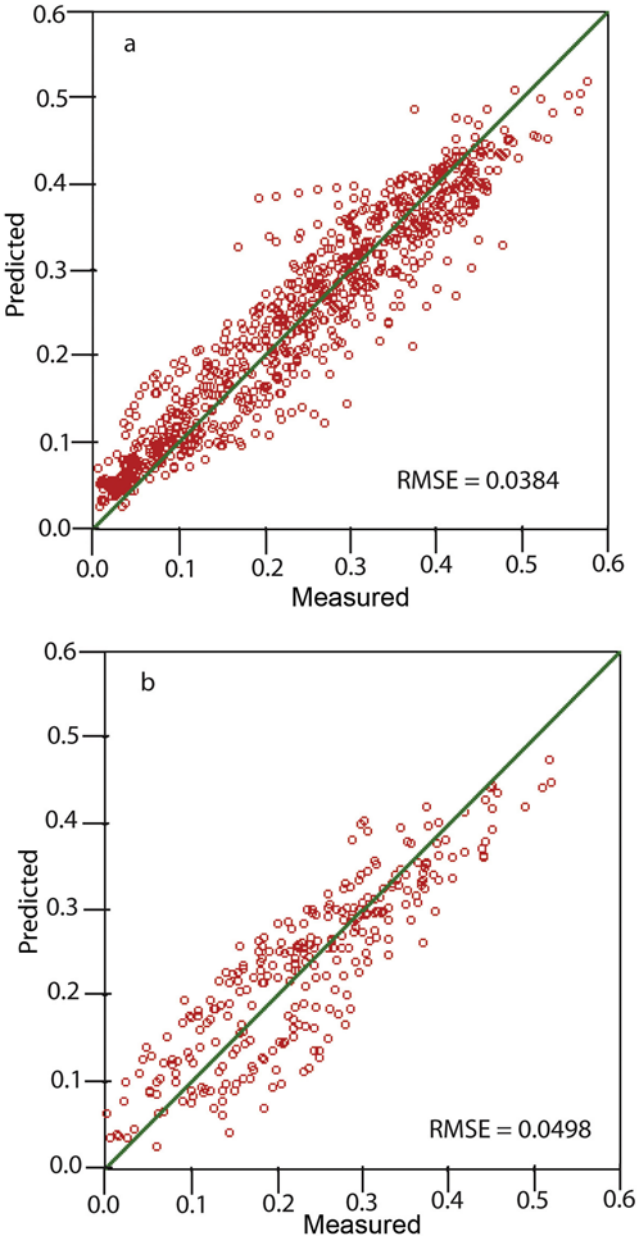

Figure 6. Neural network (a) training and (b) testing data for the UZF data set.

encouraging for the possibility of generalizing a link between a $\theta(\psi)$ and a $K(\theta)$ parameter, but not as much for the possibility of a single-parameter $K(\theta)$ relation.

[24] The neural network analysis was performed using several combinations of training and testing data sets, including the data presented here (referred to as the UZF data set) and two separate data sets chosen from the UNSODA database (Nemes et al., data set, 1999). The four training data sets were used: 100 samples from the UZF data set, 90 samples from UNSODA set 1, a combination of 50 samples from UZF data and 50 from UNSODA set 1, and 50 from UNSODA

Table 2. Correlations Between Hydraulic and Bulk Physical Properties With Transformation of Selected Variables in Terms of R^2 Values

	Sample Depth	Bulk Density	log (Geometric Mean Particle Diameter)	log (Geometric Particle-Size Standard Deviation)	log (Median Particle Diameter)	log (Uniformity Coefficient)
log (K_{sat})	0.024	0.001	0.336	0.001	0.324	0.008
log (ψ_o)	0.133	0.115	0.495	0.130	0.531	0.056
log (λ)	0.011	0.000	0.069	0.103	0.049	0.220
log (α)	0.072	0.016	0.396	0.008	0.368	0.046
Percent saturation at K = 1E-6	0.016	0.014	0.473	0.156	0.193	0.294
Percent saturation at K = 3E-8	0.035	0.004	0.572	0.024	0.533	0.152
Percent saturation at K = 5E-9	0.063	0.000	0.575	0.011	0.497	0.083

Table 3. Training and Testing Data Combinations With RMSR Values

Training Data		Testing Data			
Data Set	RMSR	UZF Data, 32 Samples	UNSODA Set 1, 90 Samples	UNSODA Set 1, 30 Samples	UNSODA Set 2, 53 Samples
UZF Data, 100 Samples	0.04	0.05	0.07		0.07
UNSODA Set 1, 90 Samples	0.02	0.10			0.05
UZF Data and UNSODA Set 1, 50 Samples Each	0.03	0.06		0.07	0.06
UNSODA Set 2, 53 Samples	0.03	0.16		0.08	

set 2 (Table 3). The error associated with the training process was similar for all four data sets, 2–4%. As expected, model testing produces higher error for all data sets, 5–16%. The training and testing results for the UZF data set (Figure 6) produce relatively low RMSR values. The highest error occurs when the UZF data set is used to test the UNSODA-trained neural network, likely due to the underrepresentation of deep unsaturated zone samples in the UNSODA data set. Training and testing the neural network with subsets of the UZF data reduces the error considerably, from 10% to 5%.

6. Conclusions

[25] High-quality unsaturated zone hydraulic property data, including unsaturated hydraulic conductivity, are desirable for use in many types of hydrologic studies including aquifer recharge estimation, habitat evaluation, determination of rainfall-runoff relations, and theoretical and property transfer model development and testing. The core sample data set presented here, which represents diverse geographic, climatic, and geomorphic environments, includes saturated and unsaturated hydraulic conductivity, water retention, particle-size distributions, and other bulk properties. All of the core samples are minimally disturbed and the measurement techniques employed are state of the art. Simple linear correlations and neural network analysis suggest relationships between bulk and hydraulic properties useful in property transfer model development.

[26] **Acknowledgments.** Funding for the work that produced this data was provided by the USGS Groundwater Resources Program, USGS National Water Quality Assessment (NAWQA) Program, USGS Toxic Substances Hydrology Programs, USGS Idaho National Laboratory Project Office in cooperation with the Department of Energy, USGS Department of the Interior Landscapes Initiative, U.S. Bureau of Reclamation, and Washington County Water Conservancy District of Utah.

References

Arya, L. M., and J. F. Paris (1981), A physicoempirical model to predict the soil moisture characteristic from particle-size distribution and bulk density data, *Soil Sci. Soc. Am. J.*, *45*(6), 1023–1030.

Brooks, R. H., and A. T. Corey (1964), Hydraulic properties of porous media, *Hydrol. Pap. 3*, 27 pp., Colo. State Univ., Fort Collins, Colo.

Campbell, G. S., and G. W. Gee (1986), Water potential: Miscellaneous methods, in *Methods of Soil Analysis, Part I—Physical and Mineralogical Methods*, *Soil Sci. Soc. Am. Book Ser.*, vol. 9, 2nd ed., edited by A. Klute, pp. 628–630, Soil Sci. Soc. of Am., Madison, Wis.

Conca, J. L., and J. Wright (1998), The UFA method for rapid, direct measurement of unsaturated transport properties in soil, sediment, and rock, *Aust. J. Soil Res.*, *36*, 291–315, doi:10.1071/S96019.

Fawcett, R. G., and N. Collis-George (1967), A filter paper method for determining the moisture characteristics of soil, *Aust. J. Exper. Agric. Animal Husbandry*, *7*(24), 162–167.

Flint, A. L., and L. E. Flint (2002), Particel density, in *Methods of Soil Analysis, Part 4—Physical Methods*, *Soil Sci. Soc. Am. Book Ser.*, vol. 5, edited by J. H. Dane and G. C. Topp, pp. 229–240, Soil Sci. Soc. of Am., Madison, Wis.

Gee, G. W., and D. Or (2002), Particle size analysis, in *Methods of Soil Analysis, Part 4—Physical Methods*, *Soil Sci. Soc. Am. Book Ser.*, vol. 5, edited by J. H. Dane and G. C. Topp, pp. 255–293, Soil Sci. Soc. of Am., Madison, Wis.

Gupta, S. C., and W. E. Larson (1979), Estimating soil water retention characteristics from particle size distribution, organic matter content, and bulk density, *Water Resour. Res.*, *15*(6), 1633–1635, doi:10.1029/WR015i006p01633.

Holtan, H. N., C. B. England, G. P. Lawless, and G. A. Schumacher (1968), Moisture-tension data for selected soils on experimental watersheds, Rep. ARS 41-144, U.S. Dep. of Agric. Agric. Res. Serv., Beltsville, Md.

Hwang, S., and S. E. Powers (2003), Lognormal distribution model for estimating soil water retention curves for sandy soils, *Soil Sci.*, *168*(3), 156–166, doi:10.1097/00010694-200303000-00002.

Minasny, B., and A. B. McBratney (2002a), The Neuro-m method for fitting neural network parametric pedotransfer functions, *Soil Sci. Soc. Am. J.*, *66*, 352–361.

Minasny, B., and A. B. McBratney (2002b), Neuropack: Neural network package for fitting pedotransfer functions, technical note, Aust. Cent. for Precis. Agric., Sydney, N. S. W., Australia.

Minasny, B., J. W. Hopmans, T. Harter, S. O. Eching, A. Tuli, and M. A. Denton (2004), Neural network prediction of soil hydraulic functions for alluvial soils using multi-step outflow data, *Soil Sci. Soc. Am. J.*, *68*, 417–429.

Morel-Seytoux, H. J., and J. R. Nimmo (1999), Soil water retention and maximum capillary drive from saturation to oven dryness, *Water Resour. Res.*, *35*, 2031–2041, doi:10.1029/1999WR900121.

Mualem, Y. (1976), A catalogue of the hydraulic properties of unsaturated soils, *Res. Proj. 442*, 118 pp., Technion Isr. Inst. of Technol., Haifa, Israel.

Nimmo, J. R., and K. C. Akstin (1988), Hydraulic conductivity of a saturated soil at low water content after compaction by various methods, *Soil Sci. Soc. Am. J.*, *52*, 303–310.

Nimmo, J. R., and K. A. Winfield (2002), Miscellaneous methods, in *Methods of Soil Analysis, Part 4—Physical Methods*, *Soil Sci. Soc. Am. Book Ser.*, vol. 5, edited by J. H. Dane and G. C. Topp, pp. 710–714, Soil Sci. Soc. of Am., Madison, Wis.

Nimmo, J. R., J. Rubin, and D. P. Hammermeister (1987), Unsaturated flow in a centrifugal field: Measurement of hydraulic conductivity and testing of Darcy's law, *Water Resour. Res.*, *23*, 124–134, doi:10.1029/WR023i001p00124.

Nimmo, J. R., D. A. Stonestrom, and K. C. Akstin (1994), The feasibility of recharge rate measurements using the steady state centrifuge method, *Soil Sci. Soc. Am. J.*, *58*, 49–56.

Nimmo, J. R., K. S. Perkins, and A. M. Lewis (2002), Steady state centrifuge, in *Methods of Soil Analysis, Part 4—Physical Methods*, *Soil Sci. Soc. Am. Book Ser.*, vol. 5, edited by J. H. Dane and G. C. Topp, pp. 903–916, Soil. Sci. Soc. of Am., Madison, Wis.

Pachepsky, Y. A., D. Timlin, and G. Varallyay (1996), Artificial neural networks to estimate soil water retention from easily measurable data, *Soil Sci. Soc. Am. J.*, *60*, 727–733.

Reynolds, W., D. Elrick, E. G. Youngs, A. Amoozegar, H. W. G. Bootlink, and J. Bouma (2002), Laboratory methods, in *Methods of Soil Analysis, Part 4—Physical Methods*, *Soil Sci. Soc. Am. Book Ser.*, vol. 5, edited by J. H. Dane and G. C. Topp, pp. 802–816, Soil. Sci. Soc. of Am., Madison, Wis.

Ross, P. J., J. Williams, and K. L. Bristow (1991), Equation for extending water-retention curves to dryness, *Soil Sci. Soc. Am. J.*, *55*, 923–927.

Rossi, C., and J. R. Nimmo (1994), Modeling of soil water retention from saturation to oven dryness, *Water Resour. Res.*, *30*(3), 701–708, doi:10.1029/93WR03238.

Schaap, M. G., and F. J. Leij (1998), Database related accuracy and uncertainty of pedotransfer functions, *Soil Sci.*, *163*, 765–779, doi:10.1097/00010694-199810000-00001.

Schaap, M. G., F. J. Leij, and M. T. van Genuchten (1998), Neural network analysis for hierarchical prediction of soil hydraulic properties, *Soil Sci. Soc. Am. J.*, *62*(4), 847–855.

van Genuchten, M. T. (1980), A closed-form equation for predicting the hydraulic conductivity of unsaturated soils, *Soil Sci. Soc. Am. J.*, *44*(5), 892–898.

Vereecken, H., J. Maes, J. Feyen, and P. Darius (1989), Estimating the soil moisture retention characteristic from texture, bulk density, and carbon content, *Soil Sci.*, *148*(6), 389–403, doi:10.1097/00010694-198912000-00001.

Vereecken, H., J. Maes, and J. Feyen (1990), Estimating unsaturated hydraulic conductivity from easily measured properties, *Soil Sci.*, *149*(1), 1–12, doi:10.1097/00010694-199001000-00001.

Wagner, B., V. R. Tarnawski, V. Hennings, U. Müller, G. Wessolek, and R. Plagge (2001), Evaluation of pedo-transfer functions for unsaturated hydraulic conductivity using an independent data set, *Geoderma*, *102*, 275–297, doi:10.1016/S0016-7061(01)00037-4.

Wösten, J. H. M., A. Lilly, A. Nemes, and C. Le Bas (1999), Development and use of a database of hydraulic properties of European soils, *Geoderma*, *90*, 169–185, doi:10.1016/S0016-7061(98)00132-3.

Young, M. H., and J. B. Sisson (2002), Tensiometry, in *Methods of Soil Analysis, Part 4—Physical Methods*, *Soil Sci. Soc. Am. Book Ser.*, vol. 5, edited by J. H. Dane and G. C. Topp, pp. 575–606, Soil Sci. Soc. of Am., Madison, Wis.

J. Nimmo and K. Perkins, U.S. Geological Survey, 345 Middlefield Road, MS 977, Menlo Park, CA 94025, USA. (kperkins@usgs.gov)